Journal of Research in Pharmacy

Research Article

www.jrespharm.com

Inhibitory effects of novel 3(2*H*)pyridazinone-triazole derivatives against acetylcholinesterase enzyme

İrem Bozbey[1*], Gülce Taşkor Önel[2], Burçin Türkmenoğlu[2], Şule Gürsoy[3], Esra Dilek[3], Muhammed Ergün[4], Azime Berna Özçelik[5], Mehtap Uysal[1]

1 Department of Pharmaceutical Chemistry, Faculty of Pharmacy, Erzincan Binali Yıldırım University, 24100 Erzincan, Turkey.
2 Department of Analytical Chemistry, Faculty of Pharmacy, Erzincan Binali Yıldırım University, 24100 Erzincan, Turkey.
3 Department of Biochemistry, Faculty of Pharmacy, Erzincan Binali Yıldırım University, 24100 Erzincan, Turkey
4 Department of Pharmaceutical Chemistry, Faculty of Pharmacy, Cumhuriyet University, Faculty of Pharmacy, 58140 Sivas, Turkey
5 Department of Pharmaceutical Chemistry, Faculty of Pharmacy, Gazi University, Ankara, 06330, Turkey
* Corresponding Author. E-mail: irem.bozbey@erzincan.edu.tr (İ.B.); Tel. +90-446-224 53 44.

Received: 30 March 2022 / Revised: 25 May 2022 / Accepted: 27 May 2022

ABSTRACT: Alzheimer's disease is a neurological disease characterized by the destruction of brain cells. In this disease, which causes a decrease in thought, memory and behavioral functions, the symptoms appear gradually with age. In this study, inhibition of acetylcholinesterase enzyme which is an important target in accordance with the cholinergic hypothesis, was studied. New 3(2*H*)pyridazinone-triazole derivatives were synthesized, confirmed by ^{1}H-NMR, ^{13}C-NMR, HRMS analysis and their IC_{50} and Ki values were studied. The inhibition constants (Ki) of the compounds against the AChE enzyme ranged from 2.35 ± 0.18 to 5.15 ± 0.46 µM. The compound with the best inhibitory properties was compound **6d** with a Ki value of 2.35 ± 0.18 µM. In addition, to support the experimental data, molecular docking studies were carried out with **6b, 6d, 6e** and **6f** compounds with AChE crystal structure (PDB ID:4M0E).

KEYWORDS: Acetylcholinesterase; alzheimer's disease; molecular docking; pyridazinone; triazole.

1. INTRODUCTION

Alzheimer's disease (AD), which affects not only the individual but also the families, is a progressive neurodegenerative disorder that affects cognition and behavior. It is stated that by 2050, more than 100 million people worldwide will be affected by Alzheimer's disease [1].

Since the emergence of AD, many primary targets have been discovered as a result of studies.

Acetylcholinesterase (AChE), beta-site amyloid precursor protein cleaving enzyme 1 (*β*-secretase, BACE-1), glycogen synthase kinase 3 beta (GSK-3β), monoamine oxidases (MAOs), metal ions in the brain, N-methyl-D-aspartate (NMDA) receptor, 5-hydroxytryptamine (5-HT) receptors, the third subtype of histamine receptor (H3 receptor), and phosphodiesterases (PDEs) are among these drug targets. Afterward, many effective compounds such as donepezil, galantamine, rivastigmine and memantine have been obtained for these drug targets. These drugs do not completely cure but are the only targeted drugs that can significantly improve the condition of patients [2].

The cholinergic hypothesis was reported in 1976 firstly [3]. It has been stated that the amount of acetylcholine (ACh) decreases in the presynaptic cholinergic terminals due to the degeneration of cholinergic neurons. The ACh in the synaptic cleft is immediately broken down into choline and acetate by AChE under 6normal physiological conditions after activating the receptors [4]. As a result of the inhibition of AChE activity, the amount of ACh is kept at a high level in the synaptic cleft. Current clinical drugs donepezil, galantamine and rivastigmine (Figure 1) are AChE inhibitors (AChEI's) [5]. Although tacrine (Figure 1) was the first AChEI to be used, it was withdrawn from treatment due to its toxicity. However, it is of great structural importance for drug design [6].

Numerous activity studies have been performed on compounds with the 3(2*H*)-pyridazinone derivatives and it has been reported that have been anticholinesterase biological activities [7-9]. Likewise, the

How to cite this article: Bozbey İ, Taşkor Önel G, Türkmenoğlu B, Gürsoy Ş, Dilek E, Ergün M, Özçelik AB, Uysal M. Inhibitory effects of novel 3(2H)pyridazinone-triazole derivatives against acetylcholinesterase enzyme. J Res Pharm. 2022; 26(5): 1461-1471.

ISSN: 2630-6344

http://dx.doi.org/10.29228/jrp.239

anticholinesterase effects of triazole structures have also been widely reported in the literature [10-13]. In the light of all this information, combination two bioactive compounds, triazole and pyridazinone, can be considered as a significant strategy for drug design and discovery. In this study, newly designed pyridazinone compounds in which the triazole ring-substituted were synthesized (Figure 2) and *in-vitro* and *in-silico* studies were performed.

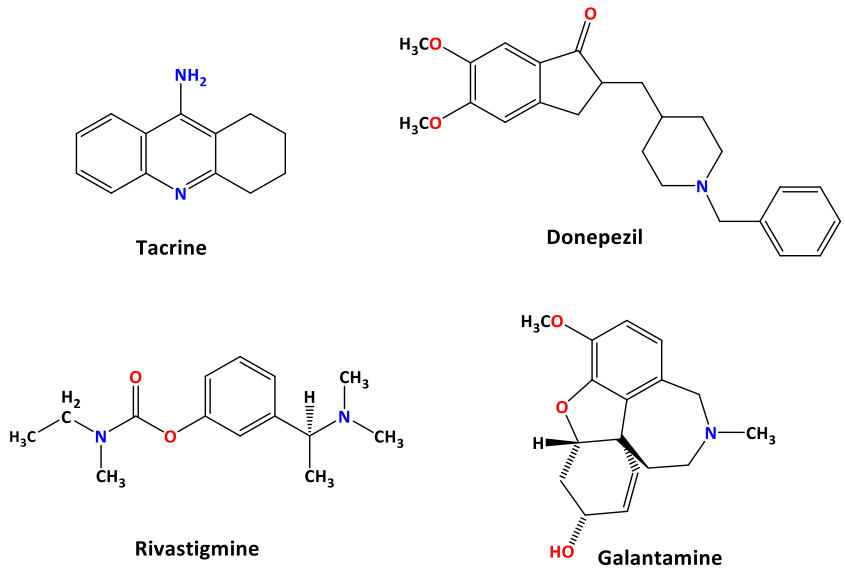

Figure 1: Structure of acetylcholinesterase inhibitors in clinical use.

2. RESULTS and DISCUSSION

In this study, new pyridazinone derivatives with thiosemicarbazide and S-triazole groups, which are expected to have AChE enzyme inhibitory effects, were synthesized and their in-vitro enzyme inhibitory activities were investigated. The synthesis diagram and the products are shown in Figure 2. The first product of reactions, 3-chloro-6-(4-(4-chlorophenyl)piperazin-1-yl)pyridazine **(1)** was obtained by the nucleophilic substitution reaction of 3,6-dichloropyridazine and 4-chlorophenylpiperazine. By heating the compound **(1)** in the glacial acetic acid solution for 6 hours, 6-[4-(4-chlorophenyl)piperazine-1-yl]-3(2*H*)-pyridazinone **(2)** was obtained. In the other step of the synthesis, the unpaired electrons of the nitrogen atom$^{(2nd)}$ of the pyridazinone group attacked the bromine-bonded carbon of ethyl 2-bromoacetate by the nucleophilic substitution S_N2 reaction mechanism to obtain the 3-substituted-6-oxopyridazynly acetate compound **(3)**. 3-substitute-6-oxopyridazynly acetato hydrazine derivative prepared to complete the heterocyclic ring system was synthesized by the reaction of the compound **(3)** and hydrazine hydrate. The final products were synthesized by the intramolecular condensation reaction of the compound **(5)** obtained as a result of the reaction of aromatic isothiocyanates and the compound **(4).**

The melting points of the white and light yellow colored compounds **6**(**a-f**), which were synthesized in yields ranging from 56-37% in general, were 229-127 ℃. The range of 14.01-13.79 ppm in the ^{1}H NMR spectrum showed triazole-N*H* peaks. Bridge of triazole and pyridazinone rings -CH_2- peak was generally observed near 5.1-4.9 ppm in proton nmr. The four protons at the 2- & 6- position of the piperazine ring were observed a doublet (*J*=10 Hz) signal in the range of 7.47-7.24 ppm, while similar protons at the 3- & 5- position were observed in the range of 7.27-6.98 ppm. In the ^{13}C NMR spectrum, the pyridazinone ring carbonyl carbon supported the structure accuracy in the range of 159.88-150.08 ppm. The specific thiocarbonyl group of triazole ring was observed in the range of 168.45-159.68 ppm. In the FT-IR spectra, newly synthesized compounds **6**(**a-f**) exhibited characteristic ν(C=O) bands at 1747-1673 cm^{-1} for pyridazinone rings. The ν(N—H) stretching bands of the triazole were centered at 3245 cm^{-1}. In addition, characteristic ν(C=S) bands observed at 1166-1151 cm^{-1}.

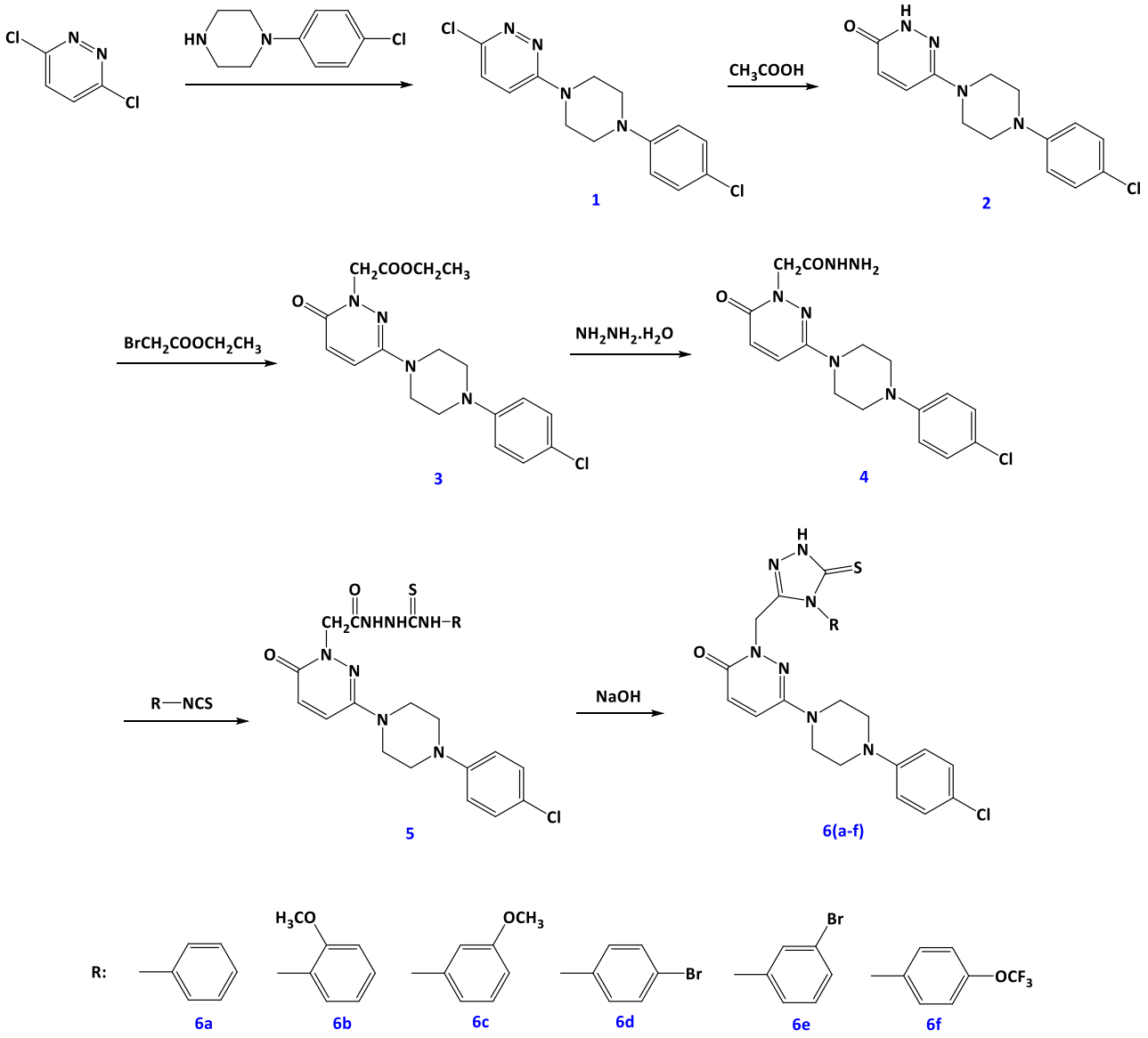

Figure 2. Synthesis diagram of the compounds (6a-f).

The structures of the resulting compounds were elucidated by ^{1}H-NMR, ^{13}C-NMR, HRMS, FT-IR methods. The peaks of the protons of the piperazine ring attached to the pyridazinone ring in the structure of the compounds were indicated as two groups.

When we examined the literature, it was observed that the anticholinesterase activity of the compounds with triazole ring structure increased compared to the reference compounds [14-16]. In our previous studies, hydrazide and hydrazone derivatives of compounds bearing pyridazinone ring were studied [8,17]. Instead of these structures, ring derivatives were designed and the inhibitory effects of the compounds in which the triazole ring was substituted were evaluated. As a result of in vivo and in vitro studies of the compounds we designed in this way, it has been determined that triazole ring substituted pyridazinone derivatives increase the activity.

The inhibitory effects of the compounds synthesized using Tacrine as the reference compound was calculated as IC_{50} and Ki (Table 1). Inhibition graphs of the most effective compound and Tacrine are given in Figure 3 and Figure 4. As a result of the AChE inhibitory activity studies of the synthesized compounds, it was determined that they showed an inhibitory effect against the enzyme. When the IC_{50} values were examined, the compound with the strongest inhibitory effect was the compound 6d with a K_i value of 2.35 ± 0.18 µM (Tacrine Ki=3.38 ± 0.25 µM). Compounds 6b, 6f, 6e, 6a and 6c, respectively, followed this compound with their

Ki (2.43 ± 0 17, 2.43 ± 0.79, 2.53 ± 0.61, 4.55 ± 1.30 5.15 ± 0.46 µM) values. When the contribution of the substituents was compared with the non-substituted compound **6a**, the 2nd substituents added to the structure increased the inhibitory effect. When 6b and 6c methoxy derivatives were examined, the presence of the methoxy group in the ortho position increased the activity. Although the position of the substituents for 6d and 6e carrying bromine did not change the activity much, the compound with -Br at the -*p* position showed a better inhibitory effect. The trifluoromethyl group at the -*p* position also increased the activity.

Table 1: The IC_{50} values, K_i constants and inhibition types of compounds (6a-f) and Tacrine (TAC)

Compounds	AChE			
	IC_{50} (µM)	R^2	Ki (µM)	Inhibition Type
6a	3.36	0.9888	4.55 ± 1.30	noncompetitive
6b	6.54	0.9232	2.43 ± 0 17	noncompetitive
6c	17.77	0.9729	5.15 ± 0.46	noncompetitive
6d	3.08	0.9857	2.35 ± 0.18	noncompetitive
6e	3.01	0.9857	2.53 ± 0.61	noncompetitive
6f	2.57	0.9924	2.43 ± 0.79	competitive
Tacrine (TAC)	4.15	0.9587	3.38 ± 0.25	competitive

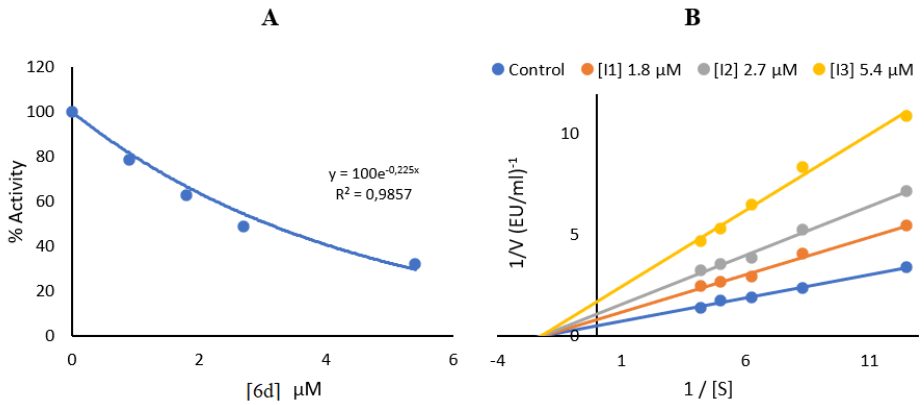

Figure 3. IC_{50} graph (A) and Lineweaver-Burk graph (B) of excellent inhibitor (6d) for AChE.

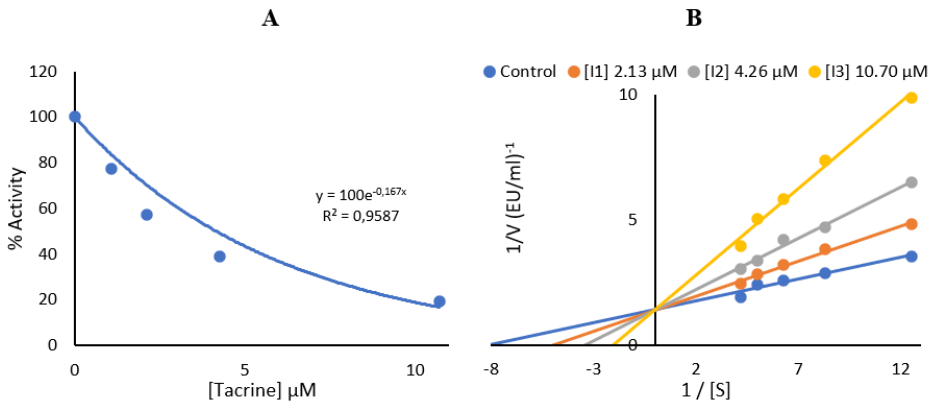

Figure 4. IC_{50} graph (A) and Lineweaver-Burk graph (B) of Tacrine (TAC) for AChE.

Molecular Docking

In molecular docking, the AChE crystal structure (PDB ID: 4M0E) obtained from the protein database was interacted with compounds **6b, 6d, 6e, 6f**, respectively, and compared with the reference drug, Tacrine. Glide score, Glide energy, Glide emodel and ΔG_{Bind}, values obtained because of molecular docking studies are given in Table 2.

Table 2: In molecular docking Glide Score, Glide Energy, Glide Emodel, ΔG_{Bind} values of the compounds with the best interaction.

Compounds	Glide Score (kcal/mol)	Glide Energy (kcal/mol)	Glide Emodel (kcal/mol)	ΔG_{Bind} (kcal/mol)
6b	-7.258	-45.082	-60.097	-54.83
6d	-7.161	-50.736	-66.607	-69.22
6e	-7.633	-44.300	-66.149	-3.86
6f	-5.213	-45.826	-63.744	-76.75
Tacrine	-6.566	-29.918	-42.832	-70.98

According to Table 2, when determining the compounds with the best binding parameter values, amino acid residues in the binding site should also be considered. Another important point in the binding parameters is the applications made with the reference drug in molecular docking. The values found because of the interaction of tacrine and 4M0E crystal structure are given in Table 2. Additionally, the 3D and 2D interaction diagram pose of the Tacrine-4M0E complex is presented in Figure 5. In Table 2, Glide Score, Glide Energy, Glide Emodel, ΔG_{Bind} energy values of tacrine were determined as -6.566, -29.918, -42.832, -70.98 kcal/mol, respectively. In line with this information, it can be said that the Glide score values of **6b, 6d** and **6f** are better than estimation. In addition, when the binding energies are examined, it can be interpreted that 6f may have a better binding than Tacrine, since it is -76.75 kcal/mol.

When Table 2 is examined, the Glide score and ΔG_{Bind} energy values of **6b** were found to be -7.258 and -54.83 kcal/mol, respectively. It is not possible to tell whether there is a good binding just by looking at the amino acids in the binding site.

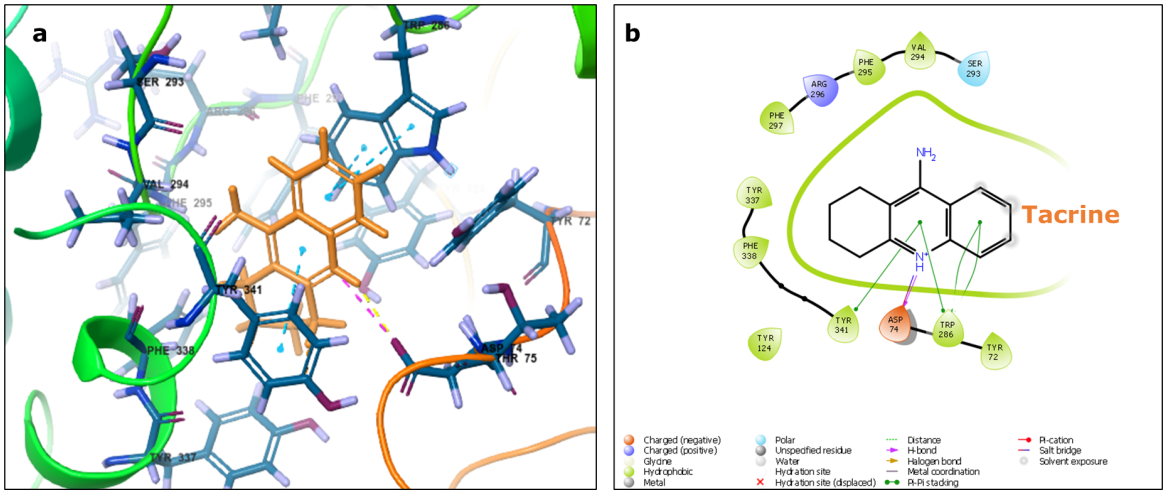

Figure 5: 3D (a) and 2D (b) representation of the interaction between the 4M0E crystal structure and Tacrine.

When the amino acid residues in the active binding region of 4M0E were analyzed in Figure 5, it was determined that Trp286 and Tyr341 had a π-π interaction and hydrogen-bonded with Asp74. In addition, it is seen in Figure 5 that Tyr72, Phe338, Tyr337, Phe295 amino acids in the active binding region have a hydrophobic interaction in binding.

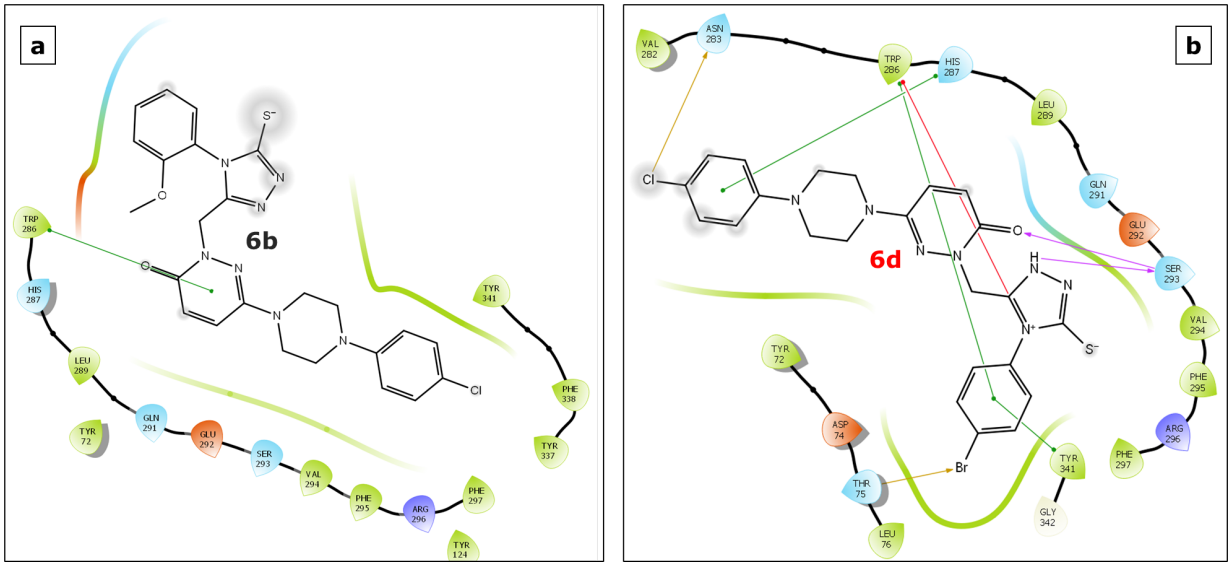

Figure 6: 2D interaction diagram poses of amino acids in the active site of 4M0E. (a) 6b, (b) 6d.

Therefore, the interaction of compounds with active amino acids at the binding site is always guided. The π-π interaction between Trp286 and **6b**, presented in Figure 6 (a), indicates that this binding can be a good lead compound in either case. The 2D interaction diagram between the AChE crystal structure (4M0E) 6d is shown in Figure 6 (b). Glide score and ΔG_{Bind} energy values were given in Table 2 as -7.161 and -69.22 kcal/mol, respectively. π-π interaction with Trp286, His287, Tyr341 amino acids, π-cation interaction with Trp286, halogen bond interaction with Asn283 and hydrogen bond interactions with Ser293 amino acid was determined.

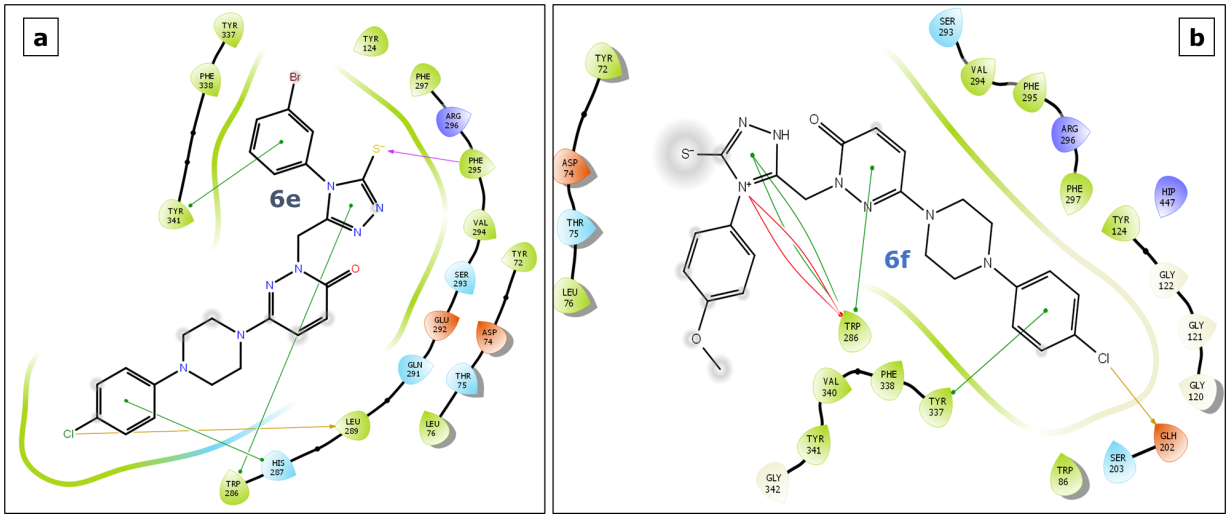

Figure 7: 2D interaction diagram poses of amino acids in the active site of 4M0E. (a) 6e, (b) 6f.

When the binding parameter values in Table 2 are analyzed, compound 6e interacting with 4M0E in molecular docking is said to be the compound with the best Glide score value. Compound 6e has a Glide score of -7.633 kcal/mol. In addition, when Figure 7(a) was examined, it is shown that it has pi-pi interaction with important amino acid residues Tyr341, H bond with Phe295, and pi-pi interactions with Trp286 and Leu289 amino acids. This indicates that ligand 6e is docked at the binding site. In Figure 7(b), the 2D interaction diagram of **6f** and 4M0E, one of the compounds with the best activity results, was shown. Figure 7 shows that the amino acid Trp286, which is one of the important amino acids in the interaction, has a π-π interaction with Trp286 from multiple sites in the 6f compound and π-π interaction with Tyr337, which is an important amino acid in the AChE structure, and with the presence of halogen bond interaction with the amino acid Glh202. It can be said that it is well docked in the active binding region in 4M0E.

3. CONCLUSION

Different 3(2*H*)pyridazinone-triazole based compounds were prepared using simple chemical reactions and they were screened for their acetylcholinesterase activity. It is thought that the *p*-position bromophenyl- supports the electron-donating effect on the 3(2*H*)-pyridazinone- triazole main structure (6d) so the chemical structure-AChE activity relationship. The arrangement of Br, Cl etc. polar groups provides electron balance on the basic structure and improves the conditions for enzyme interaction. Molecular docking studies revealed that the Glide score and ΔG_{Bind} energy values of compounds **6b, 6d, 6e** and **6f** strongly interact with the AChE enzyme. It has been determined that the used AChE interacts with the important amino acid residues Trp286 and Tyr341 in the crystal structure (PDB ID:4M0E). Molecular docking results showed that these compounds have good results comparable to Tacrine drug and can be a reference for future studies.

5. MATERIALS AND METHODS

4.1. Chemistry

Stuart SMP30 melting point apparatus was used to measure the Melting point of the compounds. Kieselgel 60 F_{254} (Merck) plates were used for controls by TLC (thin layer chromatography). NMR spectra of compounds were taken with the Bruker Avance Neo 500 MHz NMR Spectrophotometer; evaluated on the δ (ppm) scale. HRMS spectra were recorded by Agilent 6530 Accurate-Mass.

4.1.1. 3-chloro-6-(4-(4-chlorophenyl)piperazin-1-yl)pyridazine (1)

0.01 of mol of 3,6-dichloropyridazine and 0.01 mol of 1-(4-chlorophenyl)piperazine were stirred in 15 mL of ethanol by heating under reflux. The reaction medium was poured into ice water; the precipitate was filtered and purified using suitable solvents [7].

4.1.2. 6-(4-(4-chlorophenyl)piperazin-1-yl)pyridazin-3(2H)-one (2)

0.05 mol of 3-chloro-6-(4-(4-chlorophenyl)piperazin-1-yl)pyridazine were stirred in 30 mL of glacial acetic acid with heating under reflux for 6 hours [18].

4.1.3. Ethyl 2-(3-(4-(4-chlorophenyl)piperazin-1-yl)-6-oxopyridazin-1(6H)-yl)acetate (3)

0.01 mol of 6-(4-(4-chlorophenyl)piperazin-1-yl)pyridazin-3(2*H*)-one, 0.02 mol of ethyl bromoacetate and 0.02 mol of potassium carbonate were mixed in 40 mL of acetone by heating under reflux for 24 hours. The mixture was cooled, the precipitated salt was filtered off and the acetone was evaporated [8].

4.1.4. 2-(3-(4-(4-chlorophenyl)piperazin-1-yl)-6-oxopyridazin-1(6H)-yl)acetohydrazide (4)

0.01 mol of ethyl 2-(3-(4-(4-chlorophenyl)piperazin-1-yl)-6-oxopyridazin-1(6*H*)-yl)acetate was dissolved in 25 mL of ethanol and 3 mL of hydrazine hydrate was added. The reaction medium was stirred at room temperature for 3 hours. The precipitate formed was filtered, washed with water, dried and purified by crystallization from suitable solvents [8].

4.1.5. Synthesis of result compounds

0.01 mol of 2-(3-(4-(4-chlorophenyl)piperazin-1-yl)-6-oxopyridazin-1(6*H*)-yl)acetohydrazide and 0.01 mol of aryl isothiocyanate were mixed in 25 mL of anhydrous ethanol by heating under reflux for varying times. The reaction medium was cooled; the precipitate was filtered off, washed with ether and dried. Thiosemicarbazide derivatives (0.01 mol) and 2% aqueous NaOH solution (20 mL) were refluxed for 2-3 hours. The reaction was cooled and neutralized with dilute HCl. The precipitate was filtered and then crystallized from ethanol [19].

*6-(4-(4-chlorophenyl)piperazin-1-yl)-2-((4-phenyl-5-thioxo-4,5-dihydro-1H-1,2,4-triazol-3-yl)methyl)pyridazin-3(2H)-one (**6a**)*

White solid (53% yield), mp 212-214˚C, ^{1}H NMR (500 MHz, DMSO-d_6, delta, ppm): 13.99 (*br*-s, 1H, triazole-N*H*), 7.45 (d, 1H, *J*=10 Hz, 5-C*H*), 7.42-7.23 (m, 5H, Ph-*H*) 7.41 (d, 2H, *J*=10 Hz, 2'''- & 6'''-C*H*), 7.02 (d, 2H, *J*=10 Hz, 3'''- & 5'''-C*H*), 6.66 (d, 1H, *J*=10 Hz, 4-C*H*), 5.03 (s, 2H, -CH_2-), 3.24 (t, 4H, 2''- & 6''-CH_2-, b+b'), 3.20 (t, 4H, 3''- & 5''-CH_2-, a+a'), ^{13}C NMR (125 MHz, DMSO-d_6) 168.31 (-*C*S), 157.38 (-*C*O), 150.13, 148.86, 147.82, 130.78, 129.28, 129.11, 128.22, 126.77, 123.24, 117.74, 48.04, 46.17, 45.83, FT-IR (neat, cm^{-1}) 3062.55, 2834.75, 1673.36 (C=O), 1568.32, 1494.77, 1446.35, 1151.43 (C=S), HRMS m/z (ES$^+$) calcd for $C_{23}H_{22}ClN_7OS$ (M+H)$^+$ 480.1373, found 480.1364.

*6-(4-(4-chlorophenyl)piperazin-1-yl)-2-((4-(2-methoxyphenyl)-5-thioxo-4,5-dihydro-1H-1,2,4-triazol-3-yl)methyl)pyridazin-3(2H)-one (**6b**)*

Light yellow solid (37% yield), mp 127-129˚C, ^{1}H NMR (500 MHz, DMSO-d_6, delta, ppm):): 13.79 (*br*-s, 1H, triazole-N*H*), 7.45 (d, 1H, *J*=10 Hz, 5-C*H*), 7.38-6.91 (m, 4H, Ph-*H*), 7.24 (d, 2H, *J*=10 Hz, 2'''- & 6'''-C*H*), 7.05 (d, 2H, *J*=10 Hz, 3'''- & 5'''-C*H*), 6.62 (d, 1H, *J*=10 Hz, 4-C*H*), 4.97 (*geminal*-d, 2H, J_{HH}=-20 Hz, -CH_2-), 3.72 (s, 3H, -OCH_3), 3.32 (t, 4H, 2''- & 6''-CH_2-, b+b'), 3.19 (t, 4H, 3''- & 5''-CH_2-, a+a'), (s, 2H, -CH_2-), ^{13}C NMR (125 MHz, DMSO-d_6) 168.45 (-*C*S), 156.88 (-*C*O), 154.23, 149.61, 148.50, 131.04, 130.19, 129.32, 128.62, 126.40, 122.73, 121.30, 120.41, 117.22, 112.45, 55.74 (-OCH_3), 47.54, 45.54, FT-IR (neat, cm^{-1}) 3046.00, 2910.62, 2836.71, 1747.92 (C=O), 1576.45, 1495.08, 1449.42, 1161.44 (C=S), HRMS m/z (ES$^+$) calcd for $C_{24}H_{24}ClN_7O_2S$ (M+H)$^+$ 510.1478, found 510.1470.

*6-(4-(4-chlorophenyl)piperazin-1-yl)-2-((4-(3-methoxyphenyl)-5-thioxo-4,5-dihydro-1H-1,2,4-triazol-3-yl)methyl)pyridazin-3(2H)-one (**6c**)*

Light yellow solid (43% yield), mp 227-229˚C, ^{1}H NMR (500 MHz, DMSO-d_6, delta, ppm): 13.91 (*br*-s, 1H, triazole-N*H*), 7.45 (d, 1H, *J*=10 Hz, 5-C*H*), 7.32-6.79 (m, 4H, Ph-*H*), 7.26 (d, 2H, *J*=10 Hz, 2'''- & 6'''-C*H*), 6.98 (d, 2H, *J*=10 Hz, 3'''- & 5'''-C*H*), 6.65 (d, 1H, *J*=10 Hz, 4-C*H*), 5.06 (s, 2H, -CH_2-), 3.75 (s, 3H, -OCH_3), 3.28 (t, 4H, 2''- & 6''-CH_2-, b+b'), 3.19 (t, 4H, 3''- & 5''-CH_2-, a+a'), ^{13}C NMR (125 MHz, DMSO-d_6) 167.86 (-*C*S), 159.46 (-*C*O), 156.91, 149.64, 148.46, 147.96, 134.60, 130.30, 129.81, 128.66, 126.43, 122.78, 119.75, 117.28, 114.93, 113.20, 55.37 (-OCH_3), 47.57, 45.64, FT-IR (neat, cm^{-1}) 3164.82, 2998.06, 1738.57 (C=O), 1567.36, 1520.49, 1435.52, 1166.58 (C=S), HRMS m/z (ES$^+$) calcd for $C_{24}H_{24}ClN_7O_2S$ (M+H)$^+$ 510.1478, found 510.1472.

*2-((4-(4-bromophenyl)-5-thioxo-4,5-dihydro-1H-1,2,4-triazol-3-yl)methyl)-6-(4-(4-chlorophenyl)piperazin-1-yl)pyridazin-3(2H)-one (**6d**)*

White solid (56% yield), mp 203-205˚C, ^{1}H NMR (500 MHz, DMSO-d_6, delta, ppm): 14.01 (*br*-s, 1H, triazole-N*H*), 7.56 (d, 1H, *J*=10 Hz, 5-C*H*), 7.51-6.98 (m, 4H, Ph-*H*), 7.49 (d, 2H, *J*=10 Hz, 2'''- & 6'''-C*H*), 6.99 (d, 2H, *J*=10 Hz, 3'''- & 5'''-C*H*), 6.66 (d, 1H, *J*=10 Hz, 4-C*H*), 4.97 (s, 2H, -CH_2-), 3.72 (t, 4H, 2''- & 6''-CH_2-, b+b'), 3.27 (t, 4H, 3''- & 5''-CH_2-, a+a'), ^{13}C NMR (125 MHz, DMSO-d_6) 159.68 (-*C*S), 156.88 (-*C*O), 149.60, 149.51, 148.10, 146.23, 145.81, 131.04, 130.27, 130.05, 128.89, 128.60, 128.56, 125.82, 122.64, 117.16, 117.07, 116.80, 47.57, 45.67, 44.28, FT-IR (neat, cm^{-1}) 3245.05 (triazole-NH), 2962.12, 2832.43, 1687.75 (C=O), 1568.74, 1529.90, 1490.86, 1443.46, 1154.42 (C=S), HRMS m/z (ES$^+$) calcd for $C_{23}H_{21}BrClN_7OS$ (M+H)$^+$ 558.0478, found 558.0475.

*2-((4-(3-bromophenyl)-5-thioxo-4,5-dihydro-1H-1,2,4-triazol-3-yl)methyl)-6-(4-(4-chlorophenyl)piperazin-1-yl)pyridazin-3(2H)-one (**6e**)*

White solid (48% yield), mp 196-198˚C, ^{1}H NMR (500 MHz, DMSO-d_6, delta, ppm): 13.96 (s, 1H, triazole-N*H*), 7.64 (d, 1H, *J*=10 Hz, 5-C*H*), 7.60-7.00 (m, 4H, Ph-*H*), 7.28 (d, 2H, *J*=10 Hz, 2'''- & 6'''-C*H*), 7.00 (d, 2H, *J*=10 Hz, 3'''- & 5'''-C*H*), 6.66 (d, 1H, *J*=10 Hz, 4-C*H*), 5.10 (s, 2H, -CH_2-), 3.74 (t, 4H, 2''- & 6''-CH_2-, b+b'), 3.27 (t, 4H, 3''- & 5''-CH_2-, a+a'), ^{13}C NMR (125 MHz, DMSO-d_6) 159.72 (-*C*S), 157.40 (-*C*O), 150.07, 148.51, 146.78, 132.85, 131.52, 130.75, 129.15, 127.52, 126.84, 123.21, 121.86, 117.75, 117.61, 117.32, 48.12, 46.02, 44.85, FT-IR (neat, cm^{-1}) 3039.16, 2961.65, 2822.52, 1577.01, 1461.73, 1444.74, 1427.27, 1154.26 (C=S), HRMS m/z (ES$^+$) calcd for $C_{23}H_{21}BrClN_7OS$ (M+H)$^+$ 558.0478, found 558.0477.

*6-(4-(4-chlorophenyl)piperazin-1-yl)-2-((5-thioxo-4-(4-(trifluoromethoxy)phenyl)-4,5-dihydro-1H-1,2,4-triazol-3-yl)methyl)pyridazin-3(2H)-one (**6f**)*

Light yellow solid (38% yield), mp 206-208˚C, ^{1}H NMR (500 MHz, DMSO-d_6, delta, ppm): 7.57 (d, 1H, *J*=10 Hz, 5-C*H*), 7.57-7.01 (m, 4H, Ph-*H*), 7.47 (d, 2H, *J*=10 Hz, 2'''- & 6'''-C*H*), 7.27 (d, 2H, *J*=10 Hz, 3'''- & 5'''-C*H*), 7.01 (d, 1H, *J*=10 Hz, 4-C*H*), 3.34 (s, 2H, -CH_2-), 3.27 (t, 4H, 2"- & 6"-CH_2-, b+b'), 3.26 (t, 4H, 3"- & 5"-CH_2-, a+a'), ^{13}C NMR (125 MHz, DMSO-d_6) 159.72 (-*C*S), 150.08 (-*C*O), 146.80, 145.34, 131.45, 129.48, 129.15, 125.79, 123.18, 117.64, 117.41, 48.10, 44.81, FT-IR (neat, cm^{-1}) 2962.02, 2821.52, 1738.57 (C=O), 1577.72, 1461.82, 1443.32, 1166.84 (C=S), HRMS m/z (ES^{+}) calcd for $C_{24}H_{21}ClF_3N_7O_2S$ $(M+H)^{+}$ 564.1196, found 564.1185.

4.2. Acetylcholinesterase (AChE) Enzyme Inhibition Studies

AChE enzyme was supplied readily. AChE enzyme activity was determined according to the method performed by Ellman et al [20]. The AChE enzyme has two substrates, DTNB [(Ellman's Reagent) 5,5-dithio-bis-(2-nitrobenzoic acid)] and acetyltiyocholiniodate. Thiocholine is formed because of the hydrolysis of the substrates. The thiocholine formed reacts with DTNB and forms the yellow 5-thio-2-nitrobenzoate anion. This molecule gives maximum absorbance at 412 nm wavelength [21]. A percent activity versus inhibitor concentration graph was drawn for the designation of the inhibition efficacy of each of the 3(2*H*)-pyridazinone derivatives **6(a-f**) on the AChE enzyme. The IC_{50} values were obtained from these graphs. For the calculation of Ki values, three different of these compounds concentrations and five substrate concentrations were used. The study also has included, inhibition graphs of the most effective compounds which were drawn separately. The same procedures were performed for Tacrine, the standard inhibitor of the AChE enzyme, and both IC_{50} and Ki values were calculated.

4.3. Molecular Docking

Active compounds were interacted to calculate parameters such as molecular docking studies, determination of amino acid residues in the active site of the receptor in the acetylcholinesterase crystal structure, docking score values and binding energy. To explore the binding mode of the compounds was carried out using software Schrödinger Glide 2021-2, LLC New York, USA [22]. In silico molecular docking studies were carried out for **6b**, **6d**, **6e** and **6f** compounds, which were synthesized and whose AChE activities were determined experimentally. Via molecular docking studies, binding parameters such as binding energy, Glide score, docking score of compounds **6b**, **6d**, **6e** and **6f** were calculated and their active binding sites were determined. While carrying out molecular docking studies of these compounds, the following procedures were followed, respectively [23].

4.3.1. Preparation of ligands

The possible conformations of the synthesized compounds are optimized using the "Ligand preparation wizard" (Schrödinger Release 2021-2: LigPrep) [24, 25] utility of the Schrödinger 2021-2 software. With this method, a net negative change of substituents changing in each case was produced using the possible tautomeric states Epic at pH 7.0 ± 2.0 [23].

4.3.2. Determination and preparation of proteins

AChE related crystal structure was obtained from the protein database (https://www.rcsb.org/). PDB ID:4M0E [25] crystal structure was used for AChE in molecular docking studies of synthesized compounds. Proteins were prepared with the Schrödinger Release 2021-2: Protein Preparation Wizard; Epic interface of the Schrödinger 2021-2 software [23, 26]. Proteins will be prepared by sequentially performing processes including deletion of water molecules, the addition of missing side chains and hydrogen atoms, protonation states, assignment of partial charges, optimization and minimization using the OPLS-2005 force field. Next, the receptor grids of these complexes are generated with the Glide (Schrödinger Release 2021-2: Glide) [22, 26] module of the Schrödinger software, and the grid boxes are defined as a 20x20x20 Å grid box centered in the original ligand of the complex [22].

Acknowledgements: We thank Erzincan Binali Yıldırım University (Project Number: TSA-2020-664) for their financial support. The authors would like to thank Erzincan Binali Yıldırım University, Basic Sciences Application and Research Center (EBYU-EUTAM) for the Schrödinger Maestro 2021-2 program.

Author contributions: Concept – İ.B., M.U.; Design – İ.B., M.U., A.B.Ö.; Supervision – İ.B.; Resources – İ.B., M.E., A.B.Ö.; Materials – İ.B., Ş.G.; Data Collection and/or Processing – İ.B., G.T.Ö., B.T., E.D., Ş.G.; Analysis and/or Interpretation – İ.B., G.T.Ö., B.T., E.D., Ş.G.; Literature Search – İ.B., G.T.Ö., B.T.; Writing – İ.B., G.T.Ö., B.T., E.D., Ş.G.; Critical Reviews – İ.B., G.T.Ö., B.T.

Conflict of interest statement: The authors declared no conflict of interest

REFERENCES

[1] Ulep-Reed M, Saraon S, McLea S. Alzheimer Disease. The Journal for Nurse Practitioners. 2017;14. [CrossRef]

[2] Zhang P, Xu S, Zhu Z, Xu J. Multi-target design strategies for the improved treatment of Alzheimer's disease. Eur J Med Chem. 2019;176:228-47. [CrossRef]

[3] Davies P, Maloney AJ. Selective loss of central cholinergic neurons in Alzheimer's disease. Lancet. 1976;2(8000):1403. [CrossRef]

[4] Augustinsson KB, Nachmansohn D. Distinction between Acetylcholine-Esterase and Other Choline Ester-splitting Enzymes. Science. 1949;110(2847):98-9. [CrossRef]

[5] Kumar A, Singh A, Ekavali. A review on Alzheimer's disease pathophysiology and its management: an update. Pharmacol Rep. 2015;67(2):195-203. [CrossRef]

[6] Hung S-Y, Fu W-M. Drug candidates in clinical trials for Alzheimer's disease. J Biomed Sci. 2017;24(1):47-. [CrossRef]

[7] Özdemir Z, Alagöz MA, Uslu H, Karakurt A, Erikci A, Ucar G, et al. Synthesis, molecular modelling and biological activity of some pyridazinone derivatives as selective human monoamine oxidase-B inhibitors. Pharmacological Reports. 2020;72(3):692-704. [CrossRef]

[8] Bozbey İ, Özdemir Z, Uslu H, Özçelik AB, Şenol FS, Orhan İ E, et al. A Series of New Hydrazone Derivatives: Synthesis, Molecular Docking and Anticholinesterase Activity Studies. Mini Rev Med Chem. 2020;20(11):1042-60. [CrossRef]

[9] Dubey S, Bhosle PA. Pyridazinone: an important element of pharmacophore possessing broad spectrum of activity. Medicinal Chemistry Research. 2015;24(10):3579-98. [CrossRef]

[10] Antoni Krasin´ski, Zoran Radic´, Roman Manetsch, Jessica Raushel, Palmer Taylor, et al. In Situ Selection of Lead Compounds by Click Chemistry: Target-Guided Optimization of Acetylcholinesterase Inhibitors. J. Am. Chem. Soc. 2005;127:6686-6692. [CrossRef]

[11] Samanesadat Hosseini, Seied Ali Pourmousavi, Mohammad Mahdavi, Parham Taslimi. Synthesis, and in vitro biological evaluations of novel naphthoquinone conjugated to aryl triazole acetamide derivatives as potential anti-Alzheimer agents. J. Mol. Struct. 2022;1255:132229. [CrossRef]

[12] Mina Saeedi, Atefeh Maleki, Aida Iraji, Roshanak Hariri, Tahmineh Akbarzadeh et al. Synthesis and bio-evaluation of new multifunctional methylindolinone-1,2,3-triazole hybrids as anti-Alzheimer's agents. J. Mol. Struct. 2021;1229:129828. [CrossRef]

[13] Mina Saeedi, Maliheh Safavi, Elahe Karimpour-Razkenari, Mohammad Mahdavi, Najmeh Edraki, et al. Synthesis of novel chromenones linked to 1,2,3-triazole ring system:Investigation of biological activities against Alzheimer's disease. Bioorganic Chemistry. 2017;70:86–93. [CrossRef]

[14] Man Xu, Yongzhi Peng, Li Zhu, Shulin Wang, Jiayou Ji, K.P. Rakesh. Triazole derivatives as inhibitors of Alzheimer's disease: Current developments and structure-activity relationships. Eur. J. Med. Chem. 2019;180:656-672. [CrossRef]

[15] Musa Özil, Halis Türker Balaydın, Murat Şentürk. Synthesis of 5-methyl-2,4-dihydro-3H-1,2,4-triazole-3-one's aryl Schiff base derivatives and investigation of carbonic anhydrase and cholinesterase (AChE, BuChE) inhibitory properties. Bioorganic Chemistry. 2019;86:705–713. [CrossRef]

[16] Mahnaz Yazdani, Najmeh Edraki, Rashid Badri, Mehdi Khoshneviszadeh, Aida Iraji, Omidreza Firuzi. 5,6-Diphenyl triazine-thio methyl triazole hybrid as a new Alzheimer's disease modifying agents. Molecular Diversity, 2020;24:641–654. [CrossRef]

[17] Ömer Faruk Çöl, İrem Bozbey, Burçin Türkmenoğlu, Mehtap Uysal. 3(2H)-pyridazinone derivatives: Synthesis, in-silico studies, structure-activity relationship and in-vitro evaluation for acetylcholinesterase enzyme inhibition. J. Mol. Struct. 2022;1261:132970

[18] Çeçen M, Oh JM, Özdemir Z, Büyüktuncel SE, Uysal M, Abdelgawad MA, et al. Design, Synthesis, and Biological Evaluation of Pyridazinones Containing the (2-Fluorophenyl) Piperazine Moiety as Selective MAO-B Inhibitors. Molecules. 2020;25(22). [CrossRef]

[19] Wujec M, Pachuta-Stec A, Stefańska J, Kuśmierz E, Siwek A. Synthesis and Antibacterial Activity of Some New Derivatives of Thiosemicarbazide and 1,2,4-Triazole. Phosphorus, Sulfur, and Silicon and the Related Elements. 2013;188(11):1661-9.[CrossRef]

[20] Ellman GL, Courtney KD, Andres V, Featherstone RM. A new and rapid colorimetric determination of acetylcholinesterase activity. Biochemical Pharmacology. 1961;7(2):88-95. [CrossRef]

[21] Shirinzadeh H, Dilek E, Alım Z. Evaluation of Naphthalenylmethylen Hydrazine Derivatives as Potent Inhibitors on, Antiatherogenic Enzymes, Paraoxonase I and Acetylcholinesterase Activities. ChemistrySelect. 2022;7(5):e202104489. [CrossRef]

[22] Schrödinger Release 2021-2: Glide S, LLC, New York, NY, 2021.

[23] Anil DA, Aydin BO, Demir Y, Turkmenoglu B. Design, synthesis, biological evaluation and molecular docking studies of novel 1H-1, 2, 3-Triazole derivatives as potent inhibitors of carbonic anhydrase, acetylcholinesterase and aldose reductase. J Mol Struct. 2022;1257:132613 [CrossRef]

[24] Schrödinger Release 2021-2: LigPrep S, LLC, New York, NY, 2021.

[25] Cheung J, Gary EN, Shiomi K, Rosenberry TL. Structures of Human Acetylcholinesterase Bound to Dihydrotanshinone I and Territrem B Show Peripheral Site Flexibility. Acs Medicinal Chemistry Letters. 2013;4(11):1091-6. [CrossRef]

[26] Schrödinger Release 2021-2: Protein Preparation Wizard; Epik S, LLC, New York, NY, 2021; Impact, Schrödinger, LLC, New York, NY; Prime, Schrödinger, LLC, New York, NY, 2021.